

Efficient Screening of nNOS-PSD95 Uncoupling Agents Based on Radiometric Fluorescent Molecularly Imprinted Sensors

Xicheng Yang¹, Yankun Gao², Hongjuan Zhang², Hongliang Xin^{2*}

1. Jinling High School, Nanjing 210029, China.

2. Nanjing Medical University, Nanjing 211166, China.

Abstract: Novel and efficient ratiometric fluorescent molecularly imprinted sensors (RFMIS) based on epitopes were developed, which can be used for the sensitive detection of neuronal nitric oxide synthase in the screening of neuronal nitric oxide synthase-postsynaptic density95 (nNOS-PSD95) coupling inhibitors. Under appropriate conditions, the fluorescence of the carbon dots quenched with the increasing concentration of nNOS₁₋₁₃₃, while the fluorescence of the quantum dots remained unchanged. The fluorescence ratio had a good linearity in the concentration range of 0-500 ng mL⁻¹ for nNOS₁₋₁₃₃ and the determination limit was 0.14 ng mL⁻¹. Using the classical nNOS-PSD95 coupling inhibitor (ZL006) as a control, the RFMIS were used as the detector to detect the free nNOS released by Gnetol and 2,3,5,4'-tetrahydroxystilbene-2-O-β-Dglucoside from natural medicine after inhibition of nNOS-PSD95. The results have shown that the uncoupling efficiencies was consistent with co-immunoprecipitation experiments. The study provides a new idea and a new way for efficient screening of nature nNOS-PSD95 coupling inhibitors from natural medicine with the advantages of high efficiency, sensitivity and traceability.

Keywords: Molecularly Imprinted Polymers; Ratio Fluorescent Sensor; Rapid Screening; Ischemic Stroke

1. Introduction

Ischemic stroke is an important disease leading to disability and death in middle-aged and elderly people, which increases the risk of cognitive impairment and neurological dysfunction^[1,2]. Neuronal damage from stroke has been linked to the excessive activation of N-methyl-D-aspartate receptors (NMDARs) and the resulting neuronal nitric oxide synthase (nNOS) activation^[3]. To disrupt the postsynaptic density95-nNOS (PSD95-nNOS) interaction which is a downstream signaling pathway and has potential to be a better drug target, is a novel and great approach to selectively inhibiting the NMDA-PSD95-nNOS signaling pathway^[4]. In our previous experiments, always using Co-Immunoprecipitation (Co-IP) to investigate the protein coupling inhibitory activity of the screening compounds from nature medicine. However, it was found that Co-IP was complicated to operate, and the antibodies used were expensive. What's more, the coupling inhibitory activity of the coupling inhibitor in the cells cannot be directly detected^[5]. Therefore, a new uncoupling activity evaluation method should be established to simplify the operation, reduce the cost, and improve the efficiency.

Molecular imprinting is a simple and flexible strategy to generate specific identification sites which are chemically and spatially complementary to the pre-selected target molecule^[6,7]. Recently, molecularly imprinted polymers (MIPs) have been used as promising recognition elements of nanosensors because of their satisfactory selectivity, good stability and low cost. While a few fluorescents molecularly imprinted polymers have been developed for optosensing a wide variety of small organic analytes such as bisphenol A, silver ions^[8] and dibutyl phthalate^[9], the imprinting of bio-macromolecules remains a challenge because of their conformational flexibility under harsh imprinting conditions and the difficulty in removing the template from the imprinted cavities. Therefore, we have proposed ratiometric fluorescent molecularly imprinted polymer (RFMIPs) based on epitopes for the rapid detection of nNOS proteins in the screening of nNOS-PSD95 coupling inhibitors.

In this paper, RFMIPs were prepared by sol-gel polymerization with nNOS as the template and carbon dots (CDs) as the detector. The evaluation of RFMIPs such as stability, response time, selectivity, sensitivity, and adsorption capacity were

investigated to show that RFMIPs can specifically identify nNOS protein. Finally, using the classical nNOS-PSD95 coupling inhibitor (ZL006) as a control, RFMIPs were used as the detector to detect the content of nNOS in cell supernatant after the action of Gnetol and 2,3,5,4'tetrahydroxystilbene-2-O- β -D-glucoside on cells. The results have shown that the uncoupling efficiencies was consistent with co-immunoprecipitation experiments.

2. Experimental

2.1 Materials and Apparatus

Lowry protein concentration assay kit was acquired from Sangon Biotech (Shanghai, China). BCATM microprotein detection kit was obtained from Thermo Fisher Scientific (Shanghai, China). Ovalbumin (OVA), bovine serum protein (BSA) and lysozyme (Lyz) were purchased from solarbio science& technology. nNOS₁₋₁₃₃ was kindly provided by the Department of pharmacology, Nanjing Medical University (Nanjing, China). All other chemicals used in this paper were of analytical reagent grade.

The fluorescence emission spectra were measured on an F-4600 spectrofluorometer (Hitachi, Japan). All Ultraviolet-Visible (UV-Vis) spectra were achieved using a Shimadzu UV-2100 spectrophotometer. About

2.2 Synthesis and evaluation of RFMIPs

A novel RFMIPs for the selective and sensitive assay of nNOS based on epitopes was synthesized by simple sol-gel process, using CDs as sensitive signal source and CdTe quantum dots as reference. Both the ratiometric fluorescent materials and imprinted sites were located on the surface of silica. The template protein nNOS₁₋₁₃₃ was not added during the preparation of ratiometric fluorescent molecularly non-imprinted polymers (RFNIPs). The rest of the preparation was the same as RFMIPs. The specific methods of the RFMIPs synthesis will be described in detail in another article.

In order to determine the adsorption isotherm, 5 mg RFMIPs and RFNIPs were suspended in 1mL PBS with different nNOS₁₋₁₃₃ concentrations (50-700 ng mL⁻¹), respectively. RFMIPs and RFNIPs emission intensity were determined by fluorescence scanning after shaking for 40 min at room temperature. The relation between nNOS₁₋₁₃₃ concentration and $\Delta(F_{450}/F_{610})$ was plotted. $\Delta(F_{450}/F_{610})$ was calculated as formula (1):

$$\Delta(F_{450}/F_{610}) = (F_{450}/F_{610})_0 - (F_{450}/F_{610})_e \quad (1)$$

Where F_{450} and F_{610} are the fluorescence intensity at 450 nm and 610 nm respectively. $(F_{450}/F_{610})_0$ represents the fluorescence intensity ratio without protein solution, and $(F_{450}/F_{610})_e$ represents the fluorescence intensity ratio after the protein was adsorbed.

Meanwhile, the dynamic adsorption was tested by monitoring the nNOS₁₋₁₃₃ concentration in the solutions at different times (5, 10, 15, 20, 30, 40 and 50 min). The molecular selectivity of RFMIPs and RFNIPs was performed with nNOS₁₋₁₃₃ and its structurally similar compounds OVA, BSA and Lyz. All the experiments above were conducted for three times in parallel.

2.3 Fluorescence measurement conditions

All fluorescence spectra had an excitation wavelength of 360 nm and a detection wavelength in the range of 400-700 nm. The parameters of the instrument were set as follows: the voltage of the photomultiplier tube was 700 V; the scanning speed was 1200 nm min⁻¹; and the slit width was 10 nm.

2.4 Application of RFMIPs in real samples

HEK-293T cells were cultured in DMEM medium containing 5 μ g mL⁻¹ penicillin, 5 μ g mL⁻¹ streptomycin and 10% (v/v) fetal bovine serum. When the cells reached a confluence of 70-90%, the same amounts of plasmids PRK5-nNOS and pcDNA3.1-PSD95 were transfected into the cells through liposomes 6000. After 24 h, the medium was discarded, then 60 μ mol L⁻¹ ZL006, Gnetol and 2,3,5,4'tetrahydroxystilbene-2-O- β -D-glucoside were added to the petri dish respectively. The

cells were collected after 12 h and lysed with RIPA lysate, then centrifuged at 12000 r min⁻¹ for 30 min and the supernatant was collected for later use.

5 mg RFMIPs were dispersed in 1 mL the above-mentioned cell supernatant and then shook for 40 minutes at room temperature. The fluorescence intensity of RFMIPs was measured and $\Delta(F_{450}/F_{610})$ was calculated. The concentration of nNOS in the supernatant was calculated according to the linear equation and the experiment was performed for three times in parallel.

3. Results and discussion

3.1 Adsorption ability evaluation of RFMIPs

Static adsorption experiments were used to measure the fluorescence response of RFMIPs and RFNIPs in nNOS₁₋₁₃₃ (0-700 ng mL⁻¹) protein solutions. As shown in Fig. 1A, as the concentration increased, the value of $\Delta(F_{450}/F_{610})$ increased, indicating that the blotting material responded to the nNOS₁₋₁₃₃ protein solution. When the solution concentration was 400 ng mL⁻¹, the response of RFNIPs reached equilibrium, $\Delta(F_{450}/F_{610})$ was about 0.41; when the protein concentration was about 600 ng mL⁻¹, the response basically reached the maximum, $\Delta(F_{450}/F_{610})$ was about 0.86. The response of RFMIPs fluorescence signals was based on the special binding site of nNOS₁₋₁₃₃ on the imprinted polymer. Therefore, the response of RFMIPs fluorescence signals was more significant than that of RFNIPs in the same concentration of nNOS₁₋₁₃₃ protein solution.

The results of the dynamic adsorption experiments were shown in Fig. 1B. At 600 ng mL⁻¹, RFMIPs and RFNIPs had different response time to nNOS₁₋₁₃₃. The $\Delta(F_{450}/F_{610})$ of RFMIPs remained basically unchanged after 40 min, which was slightly slower than that of RFNIPs, probably because the response process of three-dimensional binding sites with complementary shapes on the surface of RFMIPs was more complicated than the random response on SMNIPs surface.

Selective fluorescence response to the template protein nNOS₁₋₁₃₃ and other protein was an important indicator to verify the successful synthesis of RFMIP. As shown in Fig. 1C, the fluorescence response of RFMIPs was about 1.5-2 times that of Lyz, OVA and BSA, while the fluorescence response of RFNIPs to each protein was not significantly different, indicating that RFMIPs could specifically recognize the template protein nNOS₁₋₁₃₃ with strong fluorescence response. This was because the surface of RFMIPs had a special binding site "tailored" for nNOS₁₋₁₃₃. nNOS₁₋₁₃₃ could bind to the site, which quenched the fluorescence intensity at 450nm and made the fluorescence ratio decrease.

3.2 Fluorescence detection mechanism

In this experiment, two kinds of fluorescent nanoparticles were introduced as detectors into molecularly imprinted polymers. For the principle of response, we proposed three possibilities based on the characteristics of the materials: (1) imprinted holes; (2) photoinduced electron transfer and (3) Foerster resonance energy transfer. The UV and fluorescence spectra were detected to further narrow the guesses. As shown in Fig. 1D, the principle of Foerster resonance energy transfer was excluded first, because there was no overlap between the UV-Vis absorption spectrum of nNOS₁₋₁₃₃ and the emission spectra of CDs and CdTe. We speculate that the fluorescence change may be caused by the photoinduced electron transfer and imprinted holes. In RFMIPs, nNOS₁₋₁₃₃ and CDs were co-imprinted in the imprinting layer. When nNOS₁₋₁₃₃ was present, it could be adsorbed by three-dimensional binding sites on the imprinted polymer through hydrogen bonding and reversible covalent bonding. After fluorescence excitation, the electrons on the conduction band of CDs in RFMIPs transitioned to the lowest unoccupied molecular orbitals unoccupied by nNOS₁₋₁₃₃ through covalent bonds or hydrogen bonds, and then directly returned to the ground state and quench the fluorescence of CDs. Thereby, the fluorescence intensity of CDs changed with the increase of nNOS₁₋₁₃₃. CdTe in RFMIPs was wrapped in the silicon layer and did not directly contact nNOS₁₋₁₃₃. It remained unchanged without photoinduced electron transfer and imprinting holes. Hence, we speculate that the detection mechanism of RFMIPs was the combined action of imprinted holes and photoinduced electron transfer.

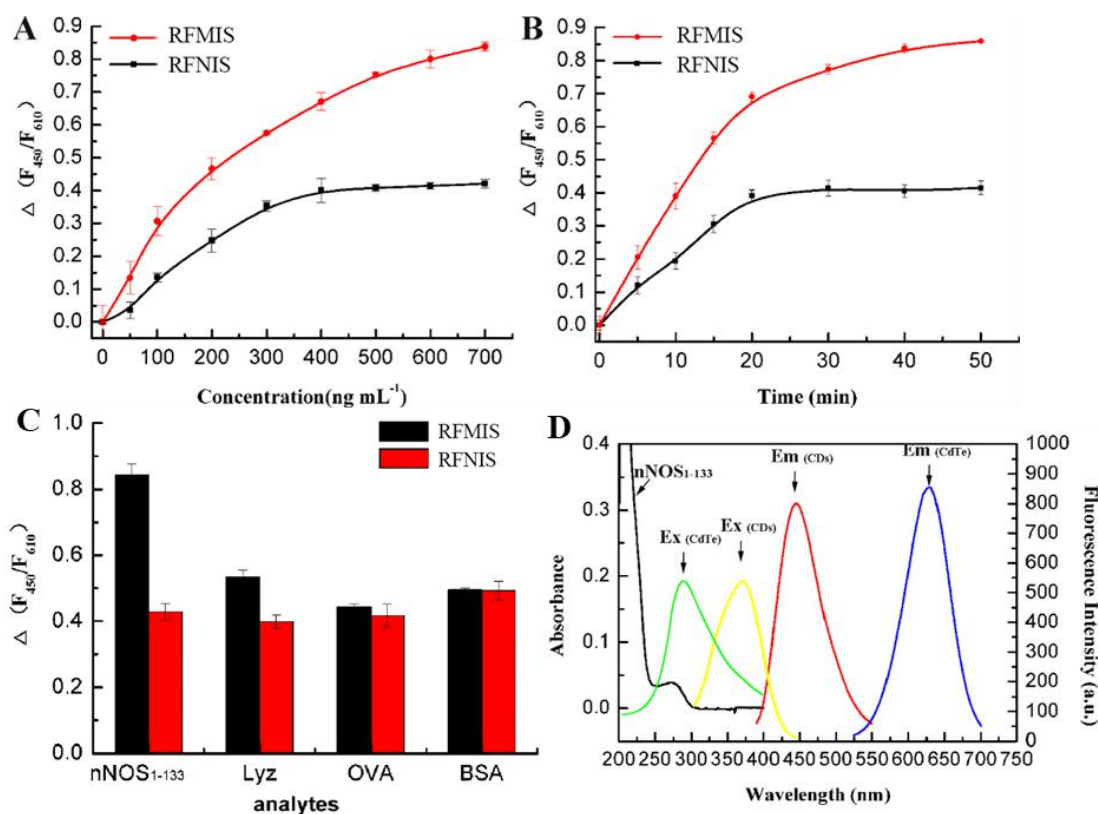


Fig. 1 (A) adsorption isotherms of RFMIPs and RFNIPs to nNOS₁₋₁₃₃, (B) adsorption kinetic curve of RFMIPs and RFNIPs to nNOS₁₋₁₃₃, (C) selective fluorescence response to nNOS₁₋₁₃₃, Lyz, OVA and BSA, (D) the UV-Vis absorption spectrum of nNOS₁₋₁₃₃ (dark line), the excitation (green line) and emission (blue line) fluorescence spectras of CdTe and the excitation (yellow line) and emission (red line) fluorescence spectras of CDs

3.3 Application of RFMIPs in real samples

3.3.1 Detection range and detection limit

5 mg RFMIPs were evenly dispersed in 1mL PBS, then 1mL nNOS₁₋₁₃₃ solution of different concentrations was added to make the protein concentrations of 0, 50, 100, 200, 300, 400 and 500 ng mL⁻¹, respectively. The solution was oscillated and shook at room temperature for 40 min. As shown in Fig. 2A, with the increase of the concentration of nNOS₁₋₁₃₃, the fluorescence intensity of CDs in RFMIPs quenched while CdTe QDs remained unchanged. As shown in Fig. 2B, the linear equation $y=0.0016x + 0.0604$ ($R^2=0.9843$) was obtained by linear fitting according to the relationship between $\Delta(F_{450}/F_{610})$ and the concentration. The LOD was 0.14 ng mL⁻¹ based on $3\sigma/K$, which is found superior to the reported assays for nNOS. The experiments showed that the fluorescence ratio had a good linear relationship with the concentration of nNOS₁₋₁₃₃, and the method could be used to calculate the concentration of nNOS₁₋₁₃₃.

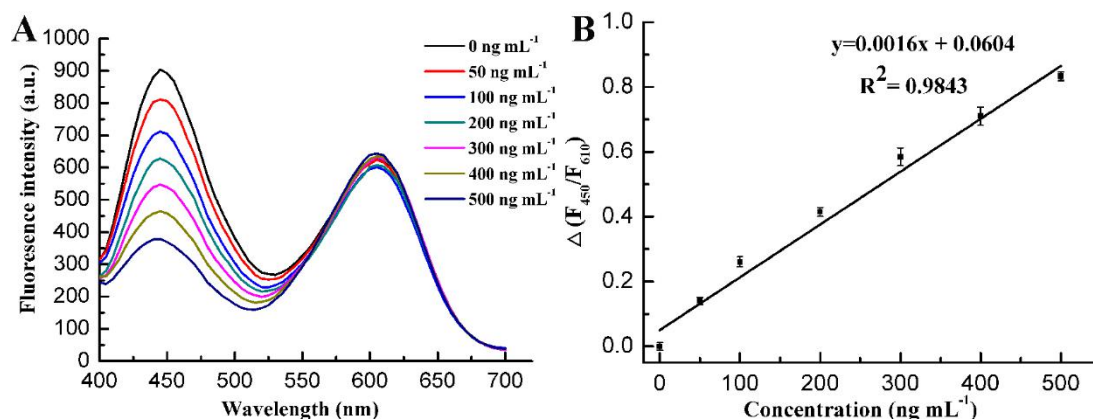


Fig. 2 (A) Fluorescence emission spectra of RFMIPs with increasing concentrations of nNOS₁₋₁₃₃; and (B) Stern-Volmer plots for the RFMIPs

3.3.2 Detection of nNOS in cells

As shown in Fig. 3A, ZL006, Gnetol and 2,3,5,4'tetrahydroxystilbene-2-O-β-D-glucoside were calculated based on the gray values of the PSD95 and nNOS bands, respectively. The coupling inhibition rate of glycosides was shown in Fig. 3B. Taking ZL006 as a reference, the coupling inhibition rate of Gnetol and 2,3,5,4'tetrahydroxystilbene-2-O-β-D-glucoside was 1.48 times and 2.17 times that of ZL006 respectively. Because nNOS₁₋₁₃₃ was the "epitope" of nNOS, RFMIPs had the ability to specifically recognize nNOS. The results of the detection of nNOS in the supernatant of cells treated with coupling inhibitors by RFMIPs were shown in Fig. 3C. The diluted supernatant reacted with ZL006, Gnetol and 2,3,5,4'tetrahydroxystilbene-2-O-β-D-glucoside containing 167.81, 233.00, and 318.35 ng mL⁻¹ nNOS protein, respectively. The uncoupling efficiencies of Gnetol and 2,3,5,4'tetrahydroxystilbene-2-O-β-D-glucoside was 1.39 and 1.90 times that of ZL006 respectively. RFMIPs could be directly used for sensitive detection of nNOS protein in supernatant without expensive magnetic bead and antibody pretreatment, which had more advantages than Western-blot for protein determination.

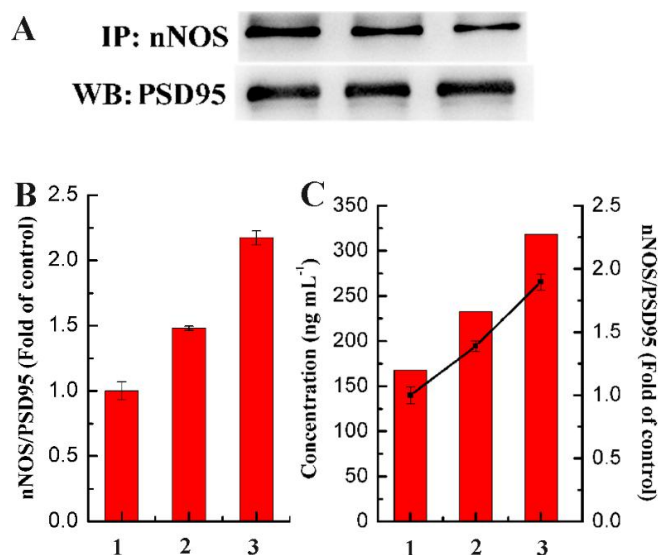


Fig. 3 Data is presented as mean±S.D. #P<0.05, compared with control. (A) the electrophoretic bands of nNOS and PSD95, (B) the coupling inhibition efficiency measured by Western-blot, (C) the concentration of nNOS and coupling inhibition efficiency measured by RFMIPs. There compounds are (1) ZL006, (2) Gnetol and (3) 2,3,5,4'-Tetrahydroxystilbene-2-O-β-D-glucoside

4. Conclusion

In this experiment, we established a method that combines the selectivity and stability of an epitope-imprinted polymer with the sensitivity of ratio fluorescence, which was used for sensitive detection of nNOS. RFMIPs were used as the detector to detect the content of nNOS in cell supernatant after the action of Gnetol and 2,3,5,4'-tetrahydroxystilbene-2-O- β -D-glucoside on cells. Compared with the content of free nNOS protein after the action of known active drug ZL006, the tests were consistent with the results of Western-blot analysis. Therefore, this experiment provides new ideas and new methods for rapid and sensitive detection of nNOS.

References

- [1] Pei, LS., Shen, X., Yan, YG., et al. The molecular mechanism of stroke treatment by Fufang Longmai Ningfang based on network pharmacology[J]. *Acta Pharmaceutica Sinica*, 2020, 55(5):898-906.
- [2] Landman, TRJ., Schoon, Y., Warle, MC., et al. Remote ischemic conditioning as an additional treatment for acute ischemic stroke: the preclinical and clinical evidence[J]. *Stroke*, 2019, 50(7):1934-1939.
- [3] Qu, WR., Liu, NK., Wu, XB., et al. Disrupting nNOS-PSD95 interaction improves neurological and cognitive recoveries after traumatic brain injury[J]. *Cerebral Cortex*, 2020, 30(7): 3859-3871.
- [4] Smith, AE., Xu, Z., Lai, YY., et al. Source memory in rats is impaired by an NMDA receptor antagonist but not by PSD95-nNOS protein-protein interaction inhibitors[J]. *Behavioural Brain Research*, 2016, 305:23-29.
- [5] Lin, JS., Lai, EM., Protein-protein interactions: Co-Immunoprecipitation. bacterial protein secretion systems[J]. *Methods Molecular Biology*, 2017, 1615:211-219.
- [6] Katz, A., Davis, ME., Molecular imprinting of bulk, microporous silica[J]. *Nature*, 2000, 403(6767): 286-289.
- [7] Pratama, KF., Manik, MER., Rahayu, D., et al. Effect of the molecularly imprinted polymer component ratio on analytical performance[J]. *Chemical and Pharmaceutical Bulletin*, 2020, 68(11):1013-1024.
- [8] S. Patra, R. Choudhary, E. Roy, et al. Triple signalling mode carbon dots-based biodegradable molecularly imprinted polymer as a multitasking visual sensor for rapid and "on-site" monitoring of silver ions[J]. *Journal of Materials Chemistry C*, 2017, 5, 11965-11976.
- [9] Zhou, ZP., Li, T., Xu, WZ., et al. Synthesis and characterization of fluorescence molecularly imprinted polymers as sensor for highly sensitive detection of dibutyl phthalate from tap water samples[J]. *Sensor Actuators B*, 2017, 240, 1114-1122.